

Molecule-Independent Electrical Switching in Pt/Organic Monolayer/Ti Devices

D. R. Stewart,* D. A. A. Ohlberg, P. A. Beck, Y. Chen, and R. Stanley Williams

Hewlett-Packard Laboratories, 1501 Page Mill Rd., Palo Alto, California 94304

J. O. Jeppesen,[†] K. A. Nielsen,[†] and J. Fraser Stoddart

Department of Chemistry and Biochemistry, UCLA, Los Angeles, California 90095

Received September 18, 2003; Revised Manuscript Received October 14, 2003

ABSTRACT

Electronic devices comprising a Langmuir–Blodgett molecular monolayer sandwiched between planar platinum and titanium metal electrodes functioned as switches and tunable resistors over a 10^2 – 10^5 Ω range under current or voltage control. Reversible hysteretic switching and resistance tuning was qualitatively similar for three very different molecular species, indicating a generic switching mechanism dominated by electrode properties or electrode/molecule interfaces, rather than molecule-specific behavior.

Molecular electronics holds the promise of scaling integrated circuits down to nanometer dimensions, if specific electrical functions can be engineered into single molecules. A large body of literature describing molecule-containing electronic devices exists; among the works most cited recently are diodes,^{1,2} voltage-activated switches,^{3–6} and negative differential resistance elements.⁷ Molecule-specific electronic switching has been reported for several of these device structures, including nanopores containing oligo(phenylene ethynylene) (OPE) monolayers^{6,7} and planar junctions incorporating rotaxane and catenane monolayers.^{3,4} However, most correlations of switching behavior with synthesized molecular properties remain speculative. In a scanning probe geometry, for example, the OPE monolayers showed only non-molecule-specific stochastic switching.⁸ The challenge of fabricating and characterizing these nanometer-scale organic/inorganic hybrid structures has meant that most devices to date contain poorly defined electrode–molecule interfaces. This is particularly true of the “solid-state” sandwich devices, where the upper electrode must be deposited on top of the organic monolayer. Theoretical transport studies highlight the significance of small changes to these interfaces.^{9–11}

Here we report a platinum/monolayer/titanium device structure that exhibits switching and well-controlled tunable resistance *independent* of molecular species. Instead of the

intended rotaxane reduction–oxidation reactions and molecular conformation changes previously reported using a silicon electrode,⁴ the device behavior in this asymmetric metal electrode sandwich is thus dominated by the electrode/organic interface properties. We suggest this generic switching mechanism may widely appear in tandem with designed molecule-specific switching, confusing efforts to interpret and reproduce the molecule-specific behaviors.

Two terminal metal/molecular-monolayer/metal planar junction devices were fabricated by sequential deposition of the bottom electrode, Langmuir–Blodgett (LB) monolayer, and top electrode on a flat insulating substrate to form 1×1 and 3×6 crossbar junction arrays.¹² The substrates were polished (100) silicon wafers capped with 200 nm of thermal SiO₂. Bottom electrodes of 100 nm thick platinum (Pt) were formed by optical lithographic techniques. Scanning electron micrographs of the Pt electrode cross-section revealed sidewalls with a minor slope from vertical and a local tapered interface to the silicon oxide. Oxygen plasma cleaning of the Pt immediately prior to LB deposition generated a thin ~ 0.4 nm platinum oxide surface.¹³ The Pt surface roughness measured by atomic force microscopy was 0.4 nm RMS over a $1 \mu\text{m}^2$ area. The static contact angle of water was 38° for the 200 nm thick thermal SiO₂ and 90° for the Pt electrode.

Three different LB monolayers were investigated: eicosanoic acid C₁₉H₃₉COOH (Aldrich) [Figure 1a] deposited as the cadmium (Cd) eicosanoate salt, an amphiphilic [2]rotaxane **R** (Figure 1c here and denoted as **I** in ref 4, where synthesis is also described), which consists of a mechanically interlocked dumbbell component and ring component, and the

* Corresponding author.

[†] Present address: Department of Chemistry, University of Southern Denmark (Odense University), Campusvej 55, DK-5230, Odense M, Denmark.

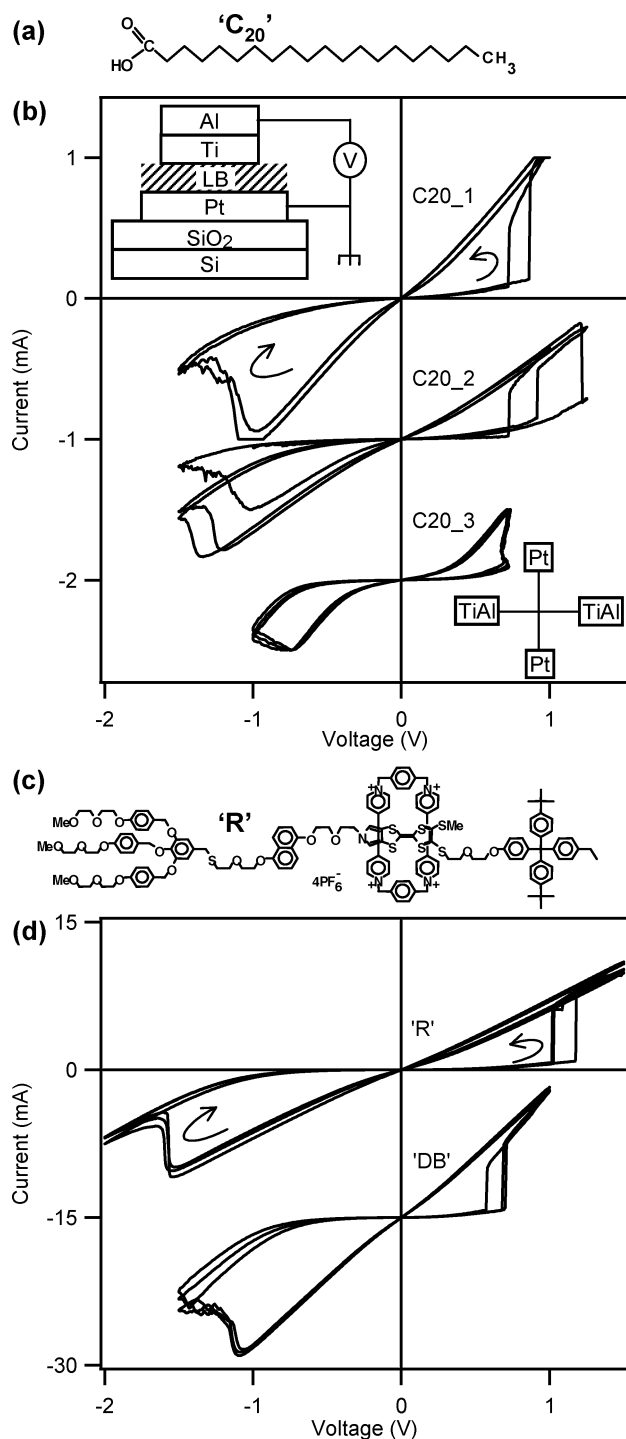


Figure 1. (a) Eicosanoic acid (C_{20}), (b) dc I - V measurements showing the “figure-8” hysteresis loops of three different C_{20} molecular monolayer devices. All sweeps follow the direction of the arrows. Successive curves are offset -1 mA. All devices are a sandwich structure of 100 nm-Pt/LB monolayer/5 nm-Ti, 200 nm-Al (inset, top). All voltages are applied w.r.t. the grounded Pt electrode. These measurements are from 1×1 junctions with planar areas of 10, 10, and $7.5 \mu\text{m}^2$ (inset, bottom). (c) [2]rotaxane **R**. The dumbbell-only molecule **DB** is identical to **R** minus the captive cyclophane ring. (d) dc voltage-bias measurements of one [2]rotaxane “**R**” device and one dumbbell “**DB**” device, of areas 25 and $50 \mu\text{m}^2$. Curves **DB** are offset -15 mA. All data at 300 K.

dumbbell-only component of **R**, labeled **DB**, which is identical to **R** except lacking the interlocked tetracationic

cyclophane ring. Eicosanoic acid was chosen as a control molecule for all our investigations because it forms well characterized, highly ordered LB films and is intrinsically an insulator. The [2]rotaxane **R** is representative of a family of molecules that incorporate intrinsic mechanical bistability (in this case cyclophane ring motion) activated by low voltage reduction–oxidation (redox) reactions.⁴ The dumbbell **DB** is a control for the bistable [2]rotaxane **R**. In previous studies by Luo et al. of different polysilicon/[2]rotaxane/titanium devices, the current–voltage (I - V) characteristics of the [2]rotaxane LB monolayer devices were reported to be molecule-specific, temperature-dependent, and correlated with solution phase redox behavior at bias magnitudes $|V| < 2$ V.⁴

During LB film deposition, the aqueous subphase was maintained at pH ~ 8.5 by the addition of tris(hydroxymethyl)aminomethane (TRIS) to typical concentrations of 10^{-4} M, at 21 °C. For the cadmium eicosanoate films, cadmium chloride was added to a concentration of 1 mM. LB transfer of the monolayers onto the Pt oxide surface is expected to produce a physisorbed molecule–electrode interface. Coordination bonding between the polar Cd eicosanoate salt and the PtO_2 is also possible though as yet unconfirmed. Ellipsometric analysis of the cadmium eicosanoate, [2]rotaxane **R**, and dumbbell **DB** monolayers yielded average film thicknesses of 2.8, 3.5, and 3.3 nm, respectively. Water contact angles were measured for the Cd eicosanoate ($109.5^\circ \pm 0.2^\circ$) and [2]rotaxane films ($90^\circ \pm 2^\circ$).

The top electrode of 5 nm titanium (Ti) + 200 nm aluminum (Al) was evaporated (e-beam, 0.1 nm/s Ti, $< 10^{-6}$ Torr) through a shadow mask onto the LB film within 1 h after monolayer deposition. Previous investigation has shown that Ti deposited onto an organic monolayer reacts aggressively with the top organic functional groups to form titanium carbon complexes; this interfacial layer prevents subsequent Ti penetration through the monolayer.¹⁴ Crossbar devices were constructed with lateral wire widths of 1–10 μm Pt and 5–20 μm Ti/Al, yielding active junction areas of 5–200 μm^2 and thus 10^7 – 10^9 molecules electrically in parallel at each junction (Figure 1b inset).

All devices were electrically characterized in ambient at 300 K or helium vapor at 4 K with 2-terminal direct current I - V sweeps under voltage-bias or current-bias. Four-probe measurements confirmed that the electrical contact resistances were $< 50 \Omega$ at all times. As fabricated, the devices exhibited an exponential I - V curve consistent with direct tunneling through an insulating film of ~ 2.5 nm thickness. This characteristic was stable for applied bias voltages between -2 V and $+1$ V (the voltage polarity convention is depicted in Figure 1b). Exceeding these limits caused an irreversible transition to a lower resistance reversible-switch state. All data presented in this work were acquired after this “forming” or “burn-in” step and describe the behavior of the reversible-switch state.

Figure 1b shows the I - V hysteresis loops of three 1×1 crosspoint Cd eicosanoate (C_{20}) devices. Each hysteresis loop is traversed as a “figure-8”, as indicated by the arrows, and can be cycled repeatedly. Two or three hysteresis cycles are

shown for each device. For example, device C20_1 of Figure 1b began in a state $R_{\text{high}} \geq 20 \text{ k}\Omega$; then application of a positive bias greater than approximately $+0.7 \text{ V}$ initiated a discrete transition to a state $R_{\text{low}} \leq 2 \text{ k}\Omega$. Both the R_{high} and R_{low} states showed nonlinear I - V characteristics, but neither curve fit a Simmons direct tunneling model.¹⁵ Continuing to negative bias exceeding approximately -1.0 V caused a rapid but continuous transition back to the R_{high} state. The bistable figure-8 hysteresis curve was reproducible, with the loop closing toward the low resistance characteristic after hundreds of cycles. Both high and low resistance states were stable to small applied voltages, $|V| < 0.1 \text{ V}$, and showed less than 0.5% change after 125 days. The positive switching threshold voltage, V_{S+} , varied in successive cycles of the same device and between devices, $+0.5 \text{ V} < V_{S+} < +1.5 \text{ V}$. The negative switching threshold voltage, V_{S-} , also varied, $-0.5 \text{ V} < V_{S-} < -2.0 \text{ V}$. The three devices of Figure 1b were measured on three different substrates, fabricated independently over a six-month period. These C₂₀ data, including variations between devices, are representative of the total 51 devices on six different substrates characterized.

Both the [2]rotaxane **R** and the rotaxane dumbbell **DB** display hysteretic behavior similar to the C₂₀ devices. Figure 1d shows one device of each molecular species, labeled “R” and “DB”, with three hysteresis cycles plotted. Current densities through the rotaxane monolayers are approximately four times higher than through the C₂₀ monolayers. Resistance ratios between rotaxane R_{high} and R_{low} states are also higher, ~ 200 for both devices in Figure 1d and reaching 10^4 in one “DB” type device. These data have been reproduced qualitatively in 65 devices on 10 different substrates fabricated over a 12-month period. A similar figure-8 hysteresis curve was also repeatedly observed on a much smaller 2500 nm^2 “R” device, comprising approximately 10^4 molecules in parallel.⁵

In Figure 2 we illustrate that each junction is in fact continuously tunable between the two extremes of high and low resistance. Beginning in the high resistance state of a C₂₀ device, successive positive current-bias sweeps to increasing maximum currents follow small counterclockwise hysteresis loops, labeled 1–7, inducing a stepwise transition from the $R_{\text{high}} \sim 1.2 \text{ k}\Omega$ to the $R_{\text{low}} \sim 250 \Omega$ state. The junction I - V characteristic remained stable at each intermediate state for low applied voltages and currents ($|V| < 0.5 \text{ V}$, $|I| < I_{\text{max}}$ of previous loop); a current bias exceeding the previous maximum positive current caused another stepwise transition toward the R_{low} state. The molecular monolayer devices thus acted as bistable resistance switches if stressed with high positive voltages as in Figure 1, and as tunable resistors if stressed by controlled positive currents, shown here. In the negative I - V quadrant, a current-bias stress caused repeatable bistable switching from the extreme R_{low} to R_{high} states. A controlled negative voltage-bias induced a tunable resistance transition from $R_{\text{low}} \sim 250 \Omega$ to $R_{\text{high}} \sim 2.1 \text{ k}\Omega$, illustrated in curves 8–17 of Figure 2. This asymmetry in controlled transitions by positive current-bias and negative voltage-bias reflects the asymmetry of the figure-8 hysteresis loop; i.e., resistance tuning controlled via

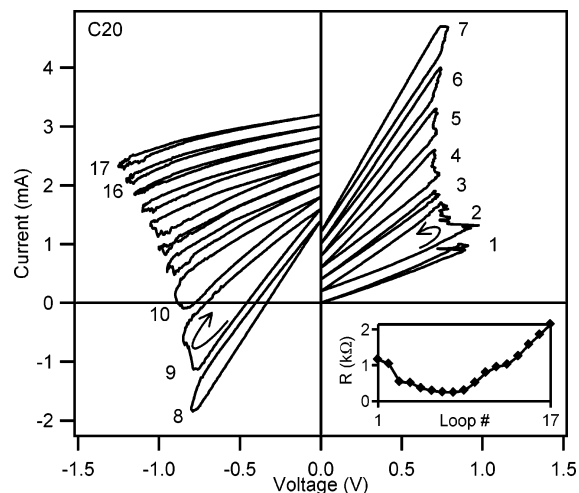


Figure 2. The resistance at $V = 0$ of a $50 \mu\text{m}^2$ C₂₀ junction is tuned continuously from $1.1 \text{ k}\Omega$ to 250Ω and back to $2.1 \text{ k}\Omega$. Data collected at $T = 4 \text{ K}$; behavior at 300 K appears identical. The tuning is achieved by applying dc current-bias sweeps toward successively higher positive currents, numbered 1–7, then dc voltage-bias sweeps toward higher negative voltages, numbered 8–17. Successive curves are offset by $+0.2 \text{ mA}$. Each positive (negative) sweep is a loop traversed counterclockwise (clockwise). Interim resistance values at $V = 0$ are plotted versus loop number (inset) and remain stable for small applied voltages $|V| < 0.5 \text{ V}$.

negative feedback to voltage, current, and power. Conversely, positive voltage-bias and negative current-bias give positive feedback and thus bistable switching. All three monolayer species displayed qualitatively similar resistance tuning behavior. Both the tuning and switching appeared independent of temperature, with apparently identical behavior at 4 and 300 K .

The remarkable asymmetry of the switching behavior (Figure 1) and the mechanism of the resistance tuning (Figure 2) are not fully understood. Symmetric¹⁶ and asymmetric¹⁷ switching have been previously observed in much larger $\sim 1 \text{ mm}^2$ LB multilayer devices, but not well explained. Previous experiments on rotaxane LB monolayer devices with polysilicon and titanium electrodes reported low-amplitude, temperature-dependent switching, correlated with specific molecular structure.⁴ Our data do not contradict these prior results. In the present investigation using Pt and Ti electrodes, the rotaxane, dumbbell, and eicosanoic acid devices all displayed high amplitude, temperature-independent switching behavior. This switching is clearly a generic property of organic monolayers within this Pt and Ti/Al electrode system. Control devices with no monolayer incorporated existed on every substrate; these devices were always metallic shorts ($< 50 \Omega$). Symmetric Pt/monolayer/Pt devices fabricated separately could be switched to lower resistance, but this switching was symmetric, i.e., polarity-independent, and irreversible. Symmetric Ti/monolayer/Ti devices have not been successfully tested; they are almost impossible to fabricate, since exposure of the metallic Ti electrode to the LB trough aqueous subphase ($> 45 \text{ min}$) always produces a Ti oxide layer. We conclude that the asymmetric switching observed in the Pt/monolayer/Ti devices arises from differences in top and bottom electrode metals (work function,

reactivity, diffusivity) or electrode-molecule interfaces (e.g., titanium-carbon complexes). The resistance tuning may result from partial reconstruction of one of these electrode surfaces, such as electromigration induced filaments,¹⁸ or incomplete electrochemical reaction of one electrode and the molecular monolayer. The deposited Ti electrode in particular is known to react with the top of the organic monolayer;¹⁴ this reaction may be driven further by the applied voltage and current stresses. The I - V curves #3-7 of Figure 2 suggest an electric field threshold for switching at $E = 0.75$ V/2.8 nm, or equivalently $E \sim 3 \times 10^6$ V/cm. Resistive power $P = I \times V$ at the point of switching is a few mW. Neither result, however, is robust across different devices in our analysis so far. While this generic switching is possibly a degradation path for molecule-specific functions, it has already proven useful in molecular electronic circuits for memory functions and logical programming including demultiplexing.^{5,12}

We have demonstrated electrical switching and resistance tuning in Pt/molecular monolayer/Ti devices. Similar hysteretic I - V characteristics were observed for three very different molecular species, striking confirmation that the electrical behavior of such molecular electronic devices is a strong function of the molecules *and* the electrodes *and* their interfacial interactions. True control of molecular device behavior is conditional upon a deeper physical understanding of this complete interacting system. Extensive physical characterization is required to ascertain the exact nature of the metal/molecule interfaces in each case; careful control experiments with substitutions of organic *and* electrode materials are required to help distinguish specific vs generic behaviors.

Acknowledgment. We gratefully acknowledge R. Baugh, C. P. Collier, M. Flores, T. Ha, S.-H. Kim, T. Kamins, P. Kuekes, S.-H. Leung, X. Li and P. Long of HP Labs and J. R. Heath, Y. Luo, and J. Perkins at UCLA for helpful discussions and assistance. We thank the Defense Advanced

Research Projects Agency in the United States and the Carlsbergfondet in Denmark for partial support.

References

- (1) Aviram, A.; Ratner, M. A. *Chem. Phys. Lett.* **1974**, *29*, 277.
- (2) Metzger, R. M. *Acc. Chem. Res.* **1999**, *32*, 950.
- (3) Collier, C. P.; Wong, E. W.; Belohradsky, M.; Raymo, F. M.; Stoddart, J. F.; Kuekes, P. J.; Williams, R. S.; Heath, J. R. *Science* **1999**, *285*, 391. Collier, C. P.; Mattersteig, G.; Wong, E. W.; Luo, Y.; Beverly, K.; Sampaio, J.; Raymo, F. M.; Stoddart, J. F.; Heath, J. R. *Science* **2000**, *289*, 1172.
- (4) Luo, Y.; Collier, C. P.; Jeppesen, J. O.; Nielsen, K. A.; DeIonno, E.; Ho, G.; Perkins, J.; Tseng, H.-R.; Yamamoto, T.; Stoddart, J. F.; Heath, J. R. *Chem. Phys. Chem.* **2002**, *3*, 519.
- (5) Chen, Y.; Jung, G. Y.; Ohlberg, D. A. A.; Li, X.; Stewart, D. R.; Williams, R. S. *Appl. Phys. Lett.* **2003**, *82*, 1620. Chen, Y.; Jung, G. Y.; Ohlberg, D. A. A.; Li, X.; Stewart, D. R.; Williams, R. S. *Nanotechnology* **2003**, *14*, 462.
- (6) Reed, M. A.; Chen, J.; Rawlett, A. M.; Price, D. W.; Tour, J. M. *Appl. Phys. Lett.* **2001**, *78*, 3735.
- (7) Chen, J.; Reed, M. A.; Rawlett, A. M.; Tour, J. M. *Science* **1999**, *286*, 1550.
- (8) Donhauser, Z. J.; Mantooh, B. A.; Kelly, K. F.; Bumm, L. A.; Monnell, J. D.; Stapleton, J. J.; Price, D. W., Jr.; Rawlett, A. M.; Allara, D. L.; Tour, J. M.; Weis, P. S. *Science* **2001**, *292*, 2303.
- (9) Xue, Y.; Datta, S.; Ratner, M. *J. Chem. Phys.* **2001**, *115*, 4292.
- (10) Kornilovich, P. E.; Bratkovsky, A. M. *Phys. Rev. B* **2001**, *64*, 195413.
- (11) Taylor, J.; Brandbyge, M.; Stokbro, K. *Phys. Rev. Lett.* **2002**, *89*, 138301.
- (12) Heath, J. R.; Kuekes, P. J.; Snider, G. S.; Williams, R. S. *Science* **1998**, *280*, 1716.
- (13) Depth profiled Auger electron spectroscopy correlated with AFM indicated a 0.3-0.4 nm PtO₂ surface layer; Beck, P. A., private communication, 2003. Li, Z.; Beck, P. A.; Ohlberg, D. A. A.; Stewart, D. R.; Williams, R. S. *Surf. Sci.* **2003**, *529*, 410.
- (14) Chang, S. C.; Li, Z.; Lau, C. N.; Larade, B.; Williams, R. S. *Appl. Phys. Lett.* **2003**, *83*, 3198. Konstantinidis, K.; Zhang, P.; Opila, R. L.; Allara, D. L. *Surf. Sci.* **1995**, *338*, 300. For a review see Jung, D. R.; Czanderna, A. W.; Herdt, G. C. *J. Vac. Sci. Technol. A* **1996**, *14*, 1779.
- (15) Simmons, J. G. *J. Appl. Phys.* **1963**, *34*, 1793.
- (16) Couch, N. R.; Montgomery, C. M. *Thin Solid Films* **1986**, *135*, 173.
- (17) Sakai, K.; Matsuda, H.; Kawade, H.; Eguchi, K.; Nakagiri, T. *Appl. Phys. Lett.* **1988**, *53*, 1274.
- (18) Recent scanning probe investigations suggest switching correlates with the formation of nanometer-scale conducting filaments; Lau, C. N.; Stewart, D. R.; Williams, R. S.; Bockrath, M., submitted 2003.

NL034795U